

Bifurcations and Chaos in Passive Walking of a Compass-Gait Biped with Asymmetries

Jae-Sung Moon and Mark W. Spong

Abstract—In this paper we study the problem of passive walking for a compass-gait biped with gait asymmetry. In particular, we identify and classify bifurcations leading to chaos caused by gait asymmetries due to unequal leg masses. We present bifurcation diagrams showing step period versus the ratio of leg masses at various walking slopes. The cell mapping method is used to find stable limit cycles as the parameters are varied. It is found that a variety of bifurcation diagrams can be grouped into six stages that consist of three expanding and three contracting stages. The analysis of each stage shows that passive dynamic walking has multiple attractors depending on initial conditions, and marginally stable limit cycles exhibit not only period doubling, but also period remerging, disconnecting, and disappearing. We also show that the rate of convergence of period doubling sequences is in good agreement with the Feigenbaum constant.

I. INTRODUCTION

Passive dynamic walking refers to the property that a suitably-designed biped can exhibit stable walking down a gentle slope without any actuation [13]. A number of studies on passive dynamic walking have been done over the years, but little is known about the effect of gait asymmetry on passive dynamic walking. Although symmetric walking is considered what we call normal walking, the study of gait asymmetry could enhance our understanding of bipedal locomotion in both robots and humans. For example, a better understanding of asymmetric walking for people with prosthetic limbs, injuries, surgical procedures, or handicaps that introduce asymmetries. In this paper, we study a compass-gait biped with asymmetric leg masses. We investigated the effect of gait asymmetry by computing bifurcation diagrams showing step periods versus bifurcation parameters.

Goswami *et al.* [6], [7] examined bifurcations as a function of ground slope in passive walking of a compass-gait biped. Period doubling bifurcations leading to a chaotic regime were observed as the slope increased. Garcia *et al.* [5] showed that a simplified walking model exhibits the same bifurcations in passive dynamic walking by plotting stance leg angles versus slope angles. Howell and Baillieul [11] used a torso-driven, as opposed to slope-driven, biped to study bifurcations and chaotic attractors. Aoi and Tsuchiya [1] used open loop sinusoidal inputs, similar to a central pattern generator, to generate periodic motions. They plotted the phase of the oscillator at each step as the constant angular velocity of the

phase varies. Both torso-driven and oscillator-driven semi-passive dynamic walking revealed period doubling bifurcations and chaotic attractors.

All of the above work on bifurcations in passive or semi-passive dynamic walking has used symmetric models with two identical legs. In the following sections, we introduce a compass-gait biped which has gait asymmetry caused by two different leg masses and derive the equations of motion. We then present a new concept of the composite hybrid system that is prerequisite for the analysis of asymmetric walking and we perform a simulation study to identify bifurcations and chaos as leg mass and slope are varied.

II. MODEL DESCRIPTION

A. The asymmetric compass-gait biped

In order to investigate gait asymmetry we utilize the compass-gait biped [6], [7] shown in Fig. 1. This two degrees of freedom biped has a hip joint connecting two straight legs and walks passively in the sagittal plane. There are no knees or torso. A hip mass is at the hip joint and two leg masses are at the centers of left and right legs. Asymmetry means the two legs are different from each other. For example, one leg is slightly longer or heavier than the other. In this paper, we primarily focus on bipeds with equal leg length but different leg masses. However, we have observed similar results to those presented here for the compass-gait with unequal leg lengths.

The movement of the compass-gait biped is divided into the swing and the impact phases. The swing phase describes that one leg is fixed on the ground as a pivot and the other leg swings above the ground while walking. These legs are called stance leg and swing leg, respectively. Since there is no external force, the total energy of the biped is conserved.

The impact phase describes the instant when the swing leg strikes the ground after passing the stance leg. When the two legs are overlapped during the swing phase the swing leg also scuffs the ground, but we ignore this touchdown in simulation. Knees or nonzero feet are required to avoid the scuffing in practice. We make the standard assumptions that the impact is perfectly inelastic and that there is no slipping at the stance foot/ground contact. In passive walking the loss of kinetic energy at impact is compensated by the increment of the potential energy gained from the change in ground slope.

B. Dynamics

The equations of motion during the swing phase can be derived from the Lagrangian dynamics. We choose the two

J. -S. Moon is with the Department of Industrial and Enterprise Systems Engineering, University of Illinois at Urbana-Champaign, Urbana, IL 61801, USA icmoon@illinois.edu

M. W. Spong is with the Department of Electrical Engineering, University of Texas at Dallas, Richardson, TX 75080, USA mspong@utdallas.edu

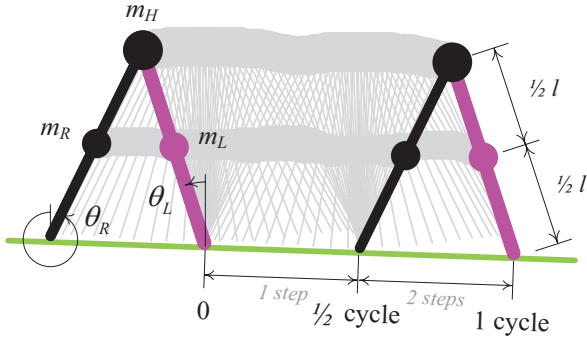


Fig. 1. A compass-gait biped and its one complete cycle of bipedal walking

leg angles θ_L and θ_R as generalized coordinates for the compass-gait biped. They are with respect to the vertical to level ground. It is important to note that gait asymmetry requires two distinct equations of motions, one with a left stance leg and the other with a right stance leg. The dynamic equations for the compass-gait biped with a left stance leg are described by [16]

$$\begin{bmatrix} M_{11} & M_{12} \\ M_{21} & M_{22} \end{bmatrix} \ddot{q} + \begin{bmatrix} 0 & C_{12} \\ C_{21} & 0 \end{bmatrix} \dot{q} + \begin{bmatrix} G_1 \\ G_2 \end{bmatrix} = 0, \quad (1)$$

where $q = [q_L, q_R]^T = [\theta_L(t), \theta_R(t)]^T$, and

$$\begin{aligned} M_{11} &= l^2(4m_H + m_L + 4m_R)/4, \\ M_{12} &= M_{21} = -l^2 m_R \cos(q_L - q_R)/2, \\ M_{22} &= l^2 m_R/4, \\ C_{12} &= -C_{21} = -l^2 m_R \sin(q_L - q_R) \dot{q}_R/2, \\ G_1 &= -gl(2m_H + m_L + 2m_R) \sin(q_L)/2, \\ G_2 &= glm_R \sin(q_R)/2. \end{aligned}$$

The other dynamic equations with a right stance leg can be derived in a similar way.

Impact dynamics are governed by conservation of angular momentum. Two distinct impact maps are also required because of the different masses of the impacting legs.

$$\dot{q}^+ = R_L(q^-) \dot{q}^-, \quad (2)$$

where superscripts $-$ and $+$ denote variables just prior to and just after impact, respectively. The impact map with a left stance leg is described by [6]

$$R_L(q^-) = \begin{bmatrix} r_{11}^+ & r_{12}^+ \\ r_{21}^+ & r_{22}^+ \end{bmatrix}^{-1} \begin{bmatrix} r_{11}^- & r_{12}^- \\ r_{21}^- & 0 \end{bmatrix}, \quad (3)$$

where

$$\begin{aligned} r_{11}^+ &= l^2(4m_H + 4m_L + m_R - 2m_L \cos(q_L^- - q_R^-))/4, \\ r_{12}^+ &= l^2 m_L (1 - 2 \cos(q_L^- - q_R^-))/4, \\ r_{21}^+ &= -l^2 m_L \cos(q_L^- - q_R^-)/2, \\ r_{22}^+ &= l^2 m_L/4, \\ r_{11}^- &= l^2(-m_L + 2(2m_H + m_L + m_R) \cos(q_L^- - q_R^-))/4, \\ r_{12}^- &= -l^2 m_R/4, \\ r_{21}^- &= -l^2 m_L/4. \end{aligned}$$

Another impact map with a right stance leg can be similarly derived.

III. SIMULATION METHODS

A. The hybrid flow of composite hybrid systems

One walking step has two phases: a continuous swing phase and a discontinuous impact phase. Let $q_L, \dot{q}_L, q_R, \dot{q}_R$ be state variables denoted by x , then state equations of each phase are given by $\dot{x} = f(x)$ and $x^+ = h(x^-)$, respectively. $f(\cdot)$ and $h(\cdot)$ with a left stance leg can be derived from (1) and (2).

One walking cycle in gait asymmetry consists of two steps for each of left and right stance leg as shown in Fig. 1, and thus its dynamics requires four state equations as follows

$$\begin{cases} \dot{x} = f_L(x), \\ x_L^+ = h_L(x_L^-), \end{cases} \quad (4)$$

$$\begin{cases} \dot{x} = f_R(x), \\ x_R^+ = h_R(x_R^-). \end{cases} \quad (5)$$

The equations (4) with a left stance leg and (5) with a right stance leg represent the composite hybrid system.

Fig. 2 illustrates the hybrid flow of a four-dimensional composite hybrid system or asymmetric walking trajectories of a compass-gait biped. Σ_L and Σ_R which are three-dimensional and transversal to the flow $\phi(x, t)$ of continuous solutions represent hyperplanes for left and right stance legs, respectively. A trajectory starting at an initial condition $x_0 \in \Sigma_L$ returns to Σ_L at x_L^- just before the right swing leg hits the ground. After touchdown, the trajectory instantaneously jumps to $x_L^+ \in \Sigma_R$ at which the second step starts. In a similar fashion, the trajectory returns to Σ_L again completing one walking cycle at x_R^+ which will be an initial condition for the next walking cycle. If a gait is symmetric walking, Σ_L and Σ_R are equivalent.

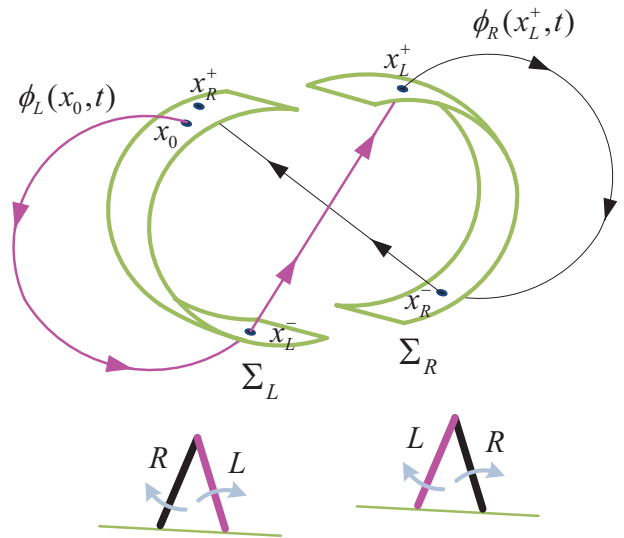


Fig. 2. The hybrid flow of a composite hybrid system. One walking cycle is represented by two continuous trajectories and two discrete jumps connecting two distinct hyperplanes.

B. Poincaré Map Method

We let x_i denote the state variable x on Σ_L after completing i cycles. If we select the hyperplane Σ_L as a Poincaré section, then the Poincaré map P is a mapping from Σ_L to Σ_L again, and can be defined by

$$x_{i+1} = P(x_i), \quad (6)$$

where $P : \Sigma_L \rightarrow \Sigma_L$ [17]. P is obtained by using the state variable x_i numerically updated from (4) and (5) every other hyperplane.

Limit cycles corresponding to walking gaits are determined by finding fixed points x^* of P . The walking cycle satisfying $x^* = P^k(x^*)$ is a period- k motion, which means $x_{i+k} = x_i$ and the cycle forms a closed orbit. k is said to be the periodicity of the limit cycle.

The stability of the limit cycle is determined using the Jacobian of the Poincaré map near fixed points, which is also numerically calculated [6], [10], [14]. The eigenvalues of the linearization all of which are inside the unit circle guarantee the orbit locally asymptotically stable.

C. Cell Mapping Method

The cell mapping method [12] is used to find limit cycles of the composite hybrid system and their periodicities. A feasible region $\mathcal{F} \subset \Sigma_L$ containing an initial condition x_0 as a starting point of cell mapping process is minced into a large number of small cell cubes whose center is located at x_0 . $Va(\cdot)$ indicates the value of the cell cube containing its state variable. Before mapping, all $Va(\cdot)$ are initialized to -1 indicating that the cell cubes are virgin cells except for the cell cube containing x_0 . We set $Va(x_0) = 0$. The mapping process starts from x_0 and proceed forward using Poincaré map function such as

$$x_0 \rightarrow P(x_0) \rightarrow P^2(x_0) \rightarrow \dots \rightarrow P^i(x_0). \quad (7)$$

At each step in generating this sequence, we need to consider the following:

- 1) If the cell cube containing a newly generated $P^i(x_0)$ is a virgin cell which means $Va(P^i(x_0)) = -1$, then we set $Va(P^i(x_0)) = i$, and move forward next mapping.
- 2) In case a newly generated $P^i(x_0)$ is out of \mathcal{F} , the original cell mapping method maps it into a sink cell and terminates the sequence. However we ignore this sequence and go on next mapping since the state variable comes back into \mathcal{F} as long as the flow is stable.
- 3) $Va(P^i(x_0)) \geq 0$ indicates that the current cell cube has encountered one of the previous sequences, and the current sequence has converged to a limit cycle. Now, this process is terminated. Suppose that the number of cycle at this moment is n , the periodicity k of the limit cycle is given by

$$k = n - Va(P^n(x_0)). \quad (8)$$

When it comes to practical considerations, the accuracy of convergence is improved by reducing the size of cell

cubes, but the smaller size of cell cubes yields the larger computation time. As for the feasible region \mathcal{F} , it is hard to choose sufficiently bulky \mathcal{F} such that $x^* \in \mathcal{F}$ at first. If a flow does not come back to \mathcal{F} in an appropriate number of cycles, x_0 should be placed at the current state variable and another mapping process resumes in a new $\tilde{\mathcal{F}} \subset \Sigma_L$.

IV. BIFURCATION DIAGRAMS

Variations of both leg masses cause gait asymmetry, and thus the mass ratio $r_m = m_R/m_L$ was used as a parameter. $r_m = 1$ means symmetric walking, that is, both legs are equivalent. As parameters of state equations are varied, bifurcations may occur in the qualitative structure of the solutions [8]. In bipedal locomotion, the bifurcations can be observed from the properties of walking cycles such as step period, walking speed, double-support angles between two legs, and so on.

We performed numerical simulations for an asymmetric compass-gait biped. All parameters except for r_m were fixed as follows: $m_H = 10$ kg, $m_{leg} = m_L + m_R = 10$ kg, $l = 1$ m. Although r_m is varied, the total mass of the system constantly maintains 20 kg since the sum of the two leg masses were fixed. As for the cell mapping method, the size of one side of a small cell cube was set to 10^{-8} and the feasible region was a 100 by 100 by 100 cube.

We calculated walking periods that elapse between Poincaré sections and the modulus of eigenvalues of the Jacobian of Poincaré maps as a function of r_m . Fig. 3 shows the two diagrams plotted in logarithmic x-axis for a 2.04 degree slope. The upper diagram is for step periods, and the lower diagram is for moduli of eigenvalues. Instead of plotting one period of walking cycle, we divided it into two periods of walking steps for left and right stance legs.

At $\ln r_m = 0.0000$ to 0.1432 , a period-1 gait appears although it shows a period-2 gait in the diagram. It is because that we chose Σ_L as a Poincaré section and thus the trajectory hits Σ_L every two steps. Two step periods are equal at $\ln r_m = 0$, but they are different when $\ln r_m$ is out of zero, which exhibits the lame walk, thus one leg

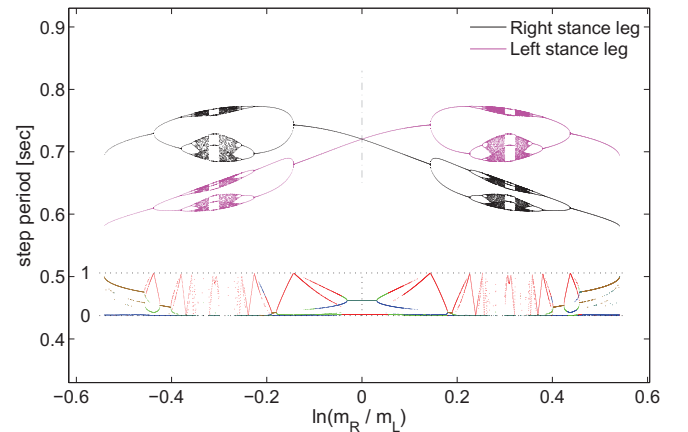
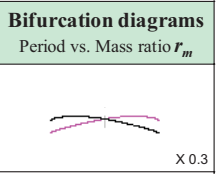
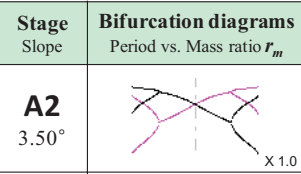
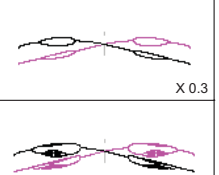
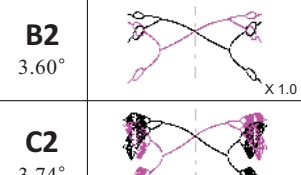
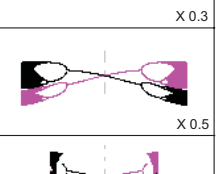

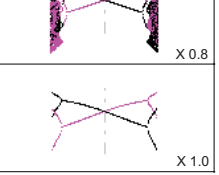

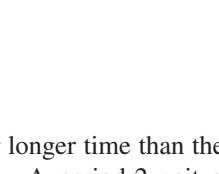
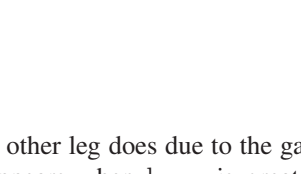
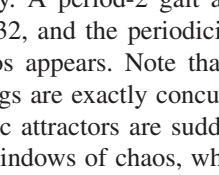
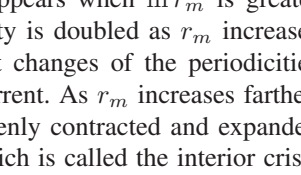


Fig. 3. A bifurcation diagram and its magnitudes of eigenvalues of the Jacobian of Poincaré maps at a 2.04 degree slope

TABLE I
SIX STAGES OF BIFURCATION DIAGRAMS

Stage Slope	Bifurcation diagrams Period vs. Mass ratio r_m	Stage Slope	Bifurcation diagrams Period vs. Mass ratio r_m
A1 0.80°	 X 0.3	A2 3.50°	 X 1.0
B1 1.90°	 X 0.3	B2 3.60°	 X 1.0
C1 2.04°	 X 0.3	C2 3.74°	 X 1.0
D1 2.10°	 X 0.5	D2 3.80°	 X 1.0
E1 2.74°	 X 0.8	E2 4.70°	 X 1.0
F1 3.00°	 X 1.0	F2 4.96°	 X 1.0

moves for longer time than the other leg does due to the gait asymmetry. A period-2 gait appears when $\ln r_m$ is greater than 0.1432, and the periodicity is doubled as r_m increases until chaos appears. Note that changes of the periodicities of both legs are exactly concurrent. As r_m increases farther, the chaotic attractors are suddenly contracted and expanded making windows of chaos, which is called the interior crisis [15], and then period remerging [2], also known as re-doubling, occurs to make the trajectories back into a period-1 gait. These walking gaits are terminated at $\ln r_m = 0.5412$ after which the biped can no longer stably walk, and then falls down. We did not plot unstable fixed points. When r_m decreases in the opposite direction, bifurcations symmetric about $\ln r_m = 0$ occur. This symmetric property at 2.04 degree slope means that the walking gait is invariant even if both leg masses are exchanged each other.

We continued to examine bifurcation diagrams by changing slopes. The lowest slope at which the stable passive dynamic walking exists was 0.03 degree, and the highest slope was 5.20 degree. We obtained the stream of bifurcations within these ranges, and each slope has its own bifurcation diagram that can be classified as one of the several distinct groups. The results were grouped into six stages as shown in table I. The bottom right corner indicates the magnification of the diagrams. In the following section, we describe the features of each stage and consider the universality that holds in all stages.

V. DISCUSSION

In symmetric walking gait, the period doubling bifurcation leading to chaos was found and it resembles stage D in table I. Our results on gait asymmetry in terms of walking slopes show the same bifurcation. Stable period-1 gaits appears from A1 to D2 at $\ln r_m = 0$ where a dotted line indicates as the slope increases. Then, a stable period-2 gait appears in E2 at $\ln r_m = 0$. It is still period-1 gait in a composite hybrid system, but period-2 gait in symmetric walking since there is only one Poincaré section. In this way, a period-4 gait appears in F2. As the slope increases, F2 moves to the right-hand side, which causes period doubling bifurcations at $\ln r_m = 0$. Finally, this process comes to an end at 5.20 degree without period remerging bifurcations.

We introduce five more stages of bifurcations exhibited in passive dynamic walking. It is known that period doubling gaits appear at the moment when the eigenvalues of the Jacobian of the Poincaré map hit the boundary of the unit circle. Thus, we examine each stage mainly focusing on the stability of periodic gaits by using the lower diagram in Fig. 3. The vertical axis indicates the modulus of the eigenvalues ranging from zero to one since only stable walking gaits were plotted.

A. Stage A

Stage A exhibits no occurrence of bifurcations but quantitative changes in it. As the slope increases, the diagram is expanding, and stable gaits take place in wider range of r_m . In case of A1 there are no changes in the periodicity of stable gaits, but the stability of the system is getting worse because the eigenvalues are approaching the boundary of the unit circle as shown in Fig. 4 (a) and (b). The moduli of the eigenvalues begin to swell around midpoints between $\ln r_m = 0$ and each end at a 1.52 degree slope, and finally Fig. 4 (c) shows that bubbles form at the place where the peak of the hump touches one. A2 has also no changes in bifurcations until increasing slopes make bubbles.

B. Stage B

Once bubbles have been formed, child bubbles are formed in the bubbles and then grandchild bubbles are consecutively formed in the child bubbles and go on spawning before chaos while diagrams are expanding with increasing slopes. In Fig. 4 (c), the most fragile regions are located at around $r_m = 0.75$ and $r_m = 1.31$ where the first bubbles appeared as a result of successions of two bifurcations, that is, period doubling and remerging, which is called period bubbling in [2]. Fig. 4 (d) shows that these bifurcations make the walking gaits more stable as the the eigenvalues in the bubbles return toward zeros. As the slope increases, new humps come out from the stabilized eigenvalues in the bubbles and they are rising again as shown in Fig. 4 (e), and finally yielding child bubbles and period-4 gaits in Fig. 4 (f). In this way consecutive period bubbling occurs from new born humps in the stabilized child bubbles repeatedly.

It is observed that the first bubble in B1 has one child bubble, but in B2, it has two child bubbles simultaneously

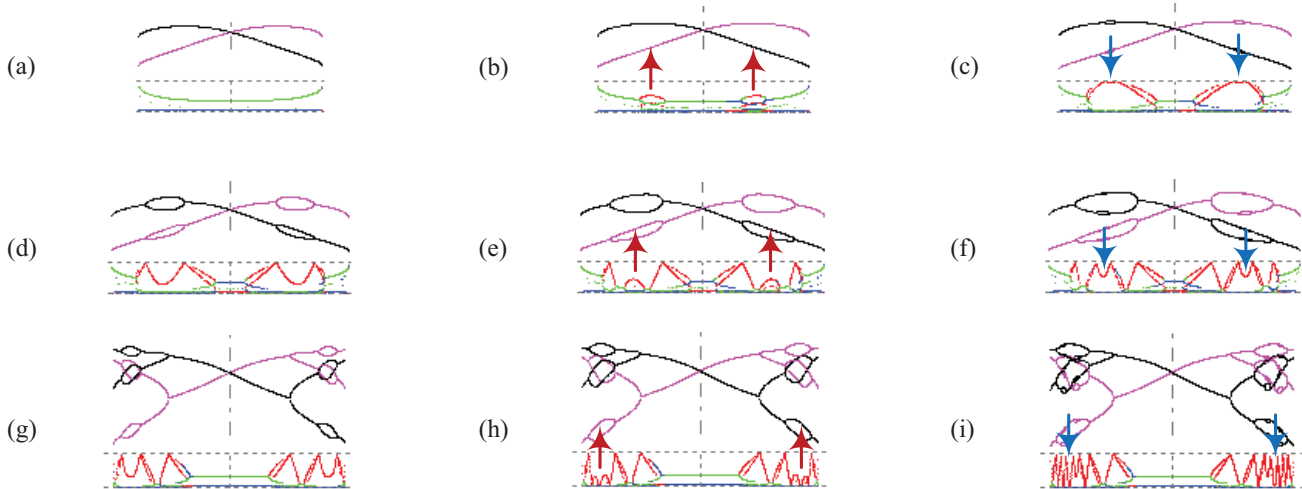


Fig. 4. Transitions between stages: (a) 1.20° slope, (b) 1.52° slope, (c) 1.76° slope, (d) 1.84° slope, (e) 1.92° slope, (f) 1.98° slope, (g) 3.60° slope, (h) 3.64° slope, and (i) 3.68° slope

formed in each branch of the first bubbles because two humps of eigenvalues rise at the same time as shown in Fig. 4 (g), (h), and (i).

C. Stage C

The bifurcation diagrams in gait asymmetry are still expanding with increasing slope after chaos has appeared in the bubbles as shown in Table I C1 and C2. Although walking gaits are still stable in chaos, we are not able to analyze the stability using eigenvalues since there are no more fixed points on the Poincaré section. The Lyapunov exponent is used to numerically analyze the chaotic attractor [9], but we did not go further.

D. Stage D

The previous three stages have been expanding so far with increasing slope. Here is the turning point at which bifurcation diagrams begin to contract. The tips in bifurcation diagram C1 and C2 indicate the borders where stable walking gaits exist. If r_m steps out of the borders, the gait is unstable and the biped falls down. As the slope increases, D1 and D2 in Table I show that all tips disappear and the regions where period remerging occurred vanish away instantly.

E. Stage E

In stage E, shrinking bifurcation diagrams are disconnected at a certain r_m and separated into two parts: the survivor and the vanisher. After D1, the regions where period-2 gaits exist are disconnected at around $r_m = 1.104$ at a 2.60 degree slope as shown in Fig. 5 (c) yielding a disconnected diagram like E1. The survivor is the middle part that consists of period-1 and period-2 gaits, and the vanishers are both extremities which include chaos. The disconnecting bifurcation occurs when a dominant eigenvalue hits the boundary of the unit circle. Fig. 5 shows that another peak stemmed from the mountainside of eigenvalues reaches one

causing disconnection. E2 also has a left part as the survivor and a right part as the vanisher.

F. Stage F

In this stage, the vanisher dwindles away at the edge between the survivor and the vanisher with increasing slope. In the end the vanisher completely disappears, but the survivor is shrunken relatively a little bit as shown in F1 and F2. After that, bifurcation diagrams begin to expand again as the slope increases.

It is notable in E2 and F2 that bifurcation diagrams are not symmetric about $\ln r_m = 0$. If we assume that exchanging leg masses does not change walking gaits, then the asymmetric diagrams imply the existence of multiple attractors. Simulation work confirmed this inference. In F2, an initial condition

$$x_1(0) = [12.2043, -66.4059, -22.1243, -7.8939][deg]$$

at $r_m = 1.005$ converges to a stable period-1 gait, but another

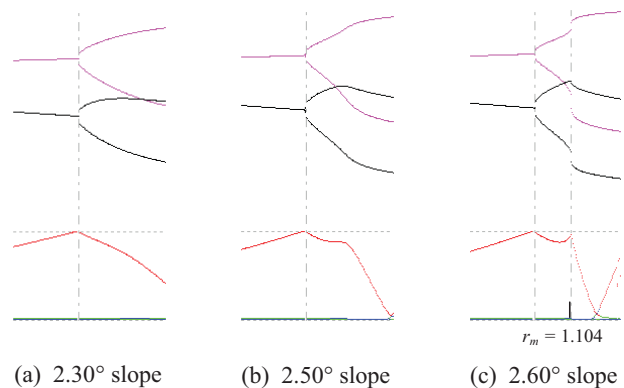


Fig. 5. Transitions from stage D to E

TABLE II
FEIGENBAUM CONSTANTS IN PASSIVE WALKING

Stage	r_m at P-16	r_m at P-32	r_m at P-64	δ
C2 3.74°	1.094313	1.094794	1.094897	4.669903
D2 3.80°	1.088440	1.088787	1.088861	4.689189
E2 4.70°	1.026028	1.026130	1.026152	4.636364
F2 4.96°	0.993703	0.993721	0.993802	4.500000

initial condition

$$x_2(0) = [14.5004, -67.8733, -24.4204, -0.3884][deg]$$

at the same r_m converges to a stable period-4 gait.

The expansion and contraction of bifurcation diagrams were observed again after F2, but we were not able to classify them as six stages.

G. Universality

In previous subsections, we have been focusing on the features of each stage. We are here concerned with the universality that holds true for all stages. Feigenbaum was the first to discover that 'the rate of convergence' of the period doubling sequences was the same between different maps [9]. Let b_n be the parameter value at which period-2ⁿ motions appear. Then

$$\delta = \lim_{n \rightarrow \infty} \frac{b_{n+1} - b_n}{b_{n+2} - b_{n+1}} \quad (9)$$

is universal with $\delta = 4.6692016091029 \dots$ [4]. We numerically calculated periodicities in each stage of C2, D2, E2, F2 up to period-64 gaits, and the rates of convergence are shown in table II. We note that there is period remerging in stage F2. Therefore we may conclude that the rate of convergence of period doubling sequences in each stage is in good agreement with the Feigenbaum delta constant.

VI. CONCLUSIONS AND FUTURE WORK

A. Conclusions

We have proposed the concept of the composite hybrid system in order to exploit the effect of gait asymmetry in bipedal locomotion. The ground slope and the mass ratio of right leg to left leg are used as bifurcation parameters, and the consecutive and repeatable types of bifurcations are calculated and grouped into six stages. The first three of them are expanding stages and the other three of them are contracting stages. The transition between stages is closely relevant to the stability of the limit cycles. We have discovered multiple attractors and the fact that passive dynamic walking exhibits four types of bifurcations: not only period doubling, but also period remerging, disconnecting, and disappearing. Furthermore, the same six stages appear in

gait asymmetry even if we use another bifurcation parameter such as the length ratio of right leg to left leg instead of the mass ratio.

B. Future Work

We are developing control laws to compensate for disparities in masses and to generate balanced and symmetric walking gaits from gait asymmetries. Ephanov and Hurmuzlu [3] have generated normal gaits of planar five link biped with gait asymmetries via swing phase control. One of the challenging issues of our model is to implement impulsive control strategies. Two different hybrid systems converge to different attractors, which can be moved to the same places by the control effort at impact phase.

REFERENCES

- [1] S. Aoi and K. Tsuchiya, "Bifurcation and chaos of a simple walking model driven by a rhythmic signal," *Int. J. Non-Linear Mech.*, vol. 41, no. 3, pp. 438–446, March 2006.
- [2] M. Bier and T. C. Bountis, "Remerging feigenbaum trees in dynamical systems," *Phys. Lett. A*, vol. 104, no. 5, pp. 239–244, September 1984.
- [3] A. Ephanov and Y. Hurmuzlu, "Generating pathological gait patterns via the use of robotic locomotion models," *Journal of Technology and Health Care*, vol. 10, pp. 135–146, 2002.
- [4] M. J. Feigenbaum, "Quantitative universality for a class of nonlinear transformations," *J. Stat. Phys.*, vol. 19, no. 1, pp. 25–52, 1978.
- [5] M. Garcia, A. Chatterjee, A. Ruina, and M. Coleman, "The simplest walking model: Stability, complexity, and scaling," *ASME J. Biomechan. Eng.*, vol. 120, pp. 281–288, 1998.
- [6] A. Goswami, B. Thuilot, and B. Espiau, "Compass-like biped robot part I: Stability and bifurcation of passive gaits," *INRIA Technical report*, no. 2996, October 1996.
- [7] —, "A study of the passive gait of a compass-like biped robot: Symmetry and chaos," *Int. J. Robot. Res.*, vol. 17, no. 12, pp. 1282–1301, 1998.
- [8] J. Guckenheimer and P. Holmes, *Nonlinear oscillations, dynamical systems, and bifurcations of vector fields*. New York: Springer-Verlag, 1986.
- [9] R. C. Hilborn, *Chaos and nonlinear dynamics: An introduction for scientists and engineers*. New York: Oxford University Press, 2000.
- [10] I. A. Hiskens, "Stability of hybrid system limit cycles: application to the compass gait biped robot," in *Proc. IEEE Conf. Decision Control*, vol. 1, pp. 774–779, Orlando, FL, December 2001.
- [11] G. W. Howell and J. Baillieul, "Simple controllable walking mechanisms which exhibit bifurcations," in *Proc. IEEE Conf. Decision Control*, pp. 3027–3032, Tampa, FL, December 1998.
- [12] C. S. Hsu, *Cell-to-cell mapping: a method of global analysis for nonlinear systems*. New York: Springer-Verlag, 1987.
- [13] T. McGeer, "Passive dynamic walking," *Int. J. Robot. Res.*, vol. 9, no. 2, pp. 62–82, 1990.
- [14] B. Morris and J. W. Grizzle, "A restricted poincar map for determining exponentially stable periodic orbits in systems with impulse effects: Application to bipedal robots," in *Proc. IEEE Conf. Decision Control*, pp. 4199–4206, Seville, Spain, December 2005.
- [15] E. Ott, *Chaos in dynamical systems*. New York: Cambridge University Press, 1993.
- [16] M. W. Spong, S. Hutchinson, and M. Vidyasagar, *Robot modeling and control*. Hoboken, NJ: Wiley, 2006.
- [17] S. H. Strogatz, *Nonlinear dynamics and Chaos: with applications to physics, biology, chemistry, and engineering*. Reading, Mass.: Addison-Wesley Pub., 1994.